

## Optical Frequency Metrology with Mode-locked Lasers

Steven T. Cundiff

JILA, National Institute of Standards and Technology and University of Colorado  
Boulder, CO, 80309-0440

At first thought, the idea of using mode-locked lasers to make a precise measurement of an optical frequency sounds really, really dumb. Mode-locked lasers make very short pulses of light, and Fourier analysis tells us that short in time means very broad in frequency, which sounds as if it provides very imprecise measurement of frequency compared, for example, to a highly stable continuous wave (cw) laser.

In actuality, mode-locked lasers are incredibly useful for optical frequency metrology. To realize why, one must remember that mode-locked lasers do not emit isolated short pulses, but rather very regularly spaced trains of short pulses. The spectrum of a pulse train consists of narrow, regularly spaced sharp peaks, resembling the teeth in a comb. This spectrum is known as a “frequency comb.” If all of the pulses emitted by the laser are identical, then it is trivial to show that the frequencies of the peaks, known as “comb lines,” are simply integer multiples of the repetition rate of the pulse train. Unfortunately, the real situation is more complicated because successive pulses emitted by the laser differ because of a mismatch between the phase and the group velocities inside the laser cavity.

The existence of the comb spectrum alone is not sufficient to make mode-locked lasers a powerful tool in optical frequency metrology. The most important fact is that the *optical*

frequencies of all of the comb lines are determined by two *radio* frequencies: the repetition rate,  $f_{rep}$ , and the offset frequency,  $f_0$ . This fact means that mode-locked laser can be used to easily connect optical frequencies with the frequency of a cesium clock, which serves as the definition of the second, and hence frequency. Furthermore, the comb spectrum provides a regularly spaced series of “tick” marks across the spectrum, allowing significantly different optical frequencies to be measured with a single apparatus. Prior to development of the techniques described in this chapter, this link was made using complex and expensive frequency chains that only measured one frequency at a time.

Optical frequency combs provide a direct link between the optical and radio-frequency regions of the electromagnetic spectrum. This fact drove the development of comb technology for use in optical frequency metrology. Although the usefulness of combs in optical frequency metrology was recognized as early as the 1970s<sup>1,2</sup> and technologies other than femtosecond lasers pursued,<sup>3</sup> the technology was not sufficient to make a direct optical-microwave link. Rather it could only be used to bridge the frequency difference between sources with similar frequencies.<sup>4</sup> The production of octave spanning combs, which allowed the measurement and control of  $f_0$ , greatly simplified optical frequency metrology.<sup>5-8</sup>

To understand why combs had such a large impact, one must ask the question, “How is the frequency of light measured?” A spectrometer might seem the logical answer. However, spectrometers are actually length-measuring devices; they measure the wavelength of light, not its frequency. An absolute measurement must be tied to the definition of the relevant unit, which for frequency is a cesium (Cs) clock. Furthermore, since length is now defined by the speed of light, a source of known frequency is needed in order to calibrate a spectrometer. Until 2000, measurement of the frequency of light was performed with complex frequency multiplication

chains,<sup>9</sup> which incorporated as many as 12 phase-locked oscillators.<sup>10</sup> These chains were complex and expensive; only a few were ever built.

Although the term “mode-locking” derives from the frequency domain description of how short pulses are produced, the details of the frequency spectrum produced by a mode-locked laser are usually glossed over. Thus this chapter starts with a derivation of the output spectrum of a mode-locked laser and its origin in the physical parameters of the laser. Based on this derivation of the spectrum, methods for measuring of the characteristic frequencies are introduced. The use of frequency combs for optical frequency metrology and optical atomic clocks follows. Finally, a few other ramifications of stabilizing the comb spectrum of a mode-locked laser are mentioned.

### **Derivation of the comb spectrum**

Ultrashort optical pulses are produced by lasers that phase lock multiple longitudinal modes in the laser cavity together so that they add up coherently at regular time intervals. The principles of mode locking are described in Chapter XX of this book. For this chapter, we do not need to worry about the mechanisms by which lasers are mode locked but will simply assume that the lasers emit a train of regularly spaced ultrashort optical pulses. The comb spectrum occurs because successive pulses interfere constructively at certain frequencies (any spectrometer with sufficient spectral resolution to distinguish the comb lines must have enough temporal dispersion that successive pulses overlap). As interference is a manifestation of the wave nature of the propagating electromagnetic field, we begin by properly describing the electric field of each pulse.

The pulses are decomposed into a carrier wave and an envelope, as depicted in Fig. 1. The carrier is a cw sinusoidal signal that is multiplied by the envelope function to produce the electric field,  $E_p(t)$ , of the pulse, i.e.,  $E_p(t) = \hat{E}(t)e^{i(\omega_c t + \phi_{ce})}$ , where  $\hat{E}(t)$  is the envelope function,  $\omega_c$  is the angular frequency of the carrier, and  $\phi_{ce}$  is the carrier-envelope phase. The square of the envelope function gives the intensity profile of the pulse. For a simple pulse, such as that shown in Fig. 1, this decomposition is straightforward and produces a simple envelope function. However, for more complicated pulses, for example a “chirped” pulse, where the frequency varies with time, the envelope function can be complex valued. In general, the decomposition into carrier and envelope is not unique. This ambiguity has been addressed with care in the context of “analytic signals”, which were originally developed to describe radar pulses. A textbook level discussion of analytic signals can be found in Chapter 3 of Mandel and Wolf.<sup>11</sup> As long as the width of the spectrum of  $E(t)$  is smaller than its mean frequency, then the intuitive choice is for  $\omega_c$  to be the mean frequency. We will soon see that the periodicity of a train of pulses imposes further restrictions on the carrier, but does not define it.

When an electromagnetic pulse propagates through a dispersive material, i.e., one where the index of refraction varies with frequency,  $\phi_{ce}$  evolves because the phase and group velocities differ. The carrier propagates at the phase velocity while the envelope propagates at the group velocity. This difference in velocities causes the carrier to “slip” through the envelope. The slipping of the carrier with respect to envelope is crucial because it occurs inside a laser cavity. This slippage means that  $\phi_{ce}$  evolves as the pulse circulates inside the laser oscillator. The phase of the intracavity pulse is sampled each time it hits the partially reflective output coupler. As a consequence,  $\phi_{ce}$  evolves from pulse to pulse in the emitted train of pulses. In the absence of

perturbations to the laser, it evolves by a fixed amount,  $\Delta\phi_{ce}$ , between successive pulses. For our purposes, it is only  $\Delta\phi_{ce}$  modulo  $2\pi$  that matters, which we will simply designate as  $\Delta\phi_{ce}$ .

As a starting point for calculating the spectrum of the pulse train, we first ignore  $\Delta\phi_{ce}$ , in which case all of the pulses are identical and we can write the electric field of the pulse train as

$$E(t) = \sum_n E_p(t - n\tau), \quad (1)$$

where  $\tau = 1/f_{rep}$  is the time between pulses; we assume that the duration of  $E_p(t)$  is less than  $\tau$ . Since  $E(t)$  is a periodic function, it can be represented as a Fourier series. Specifically, the spectrum is given by the Poisson sum formula from Fourier analysis:

$$\sum_{m=-\infty}^{\infty} f(x - mp) = \sum_{k=-\infty}^{\infty} \frac{1}{p} F\left(\frac{k}{p}\right) e^{2\pi i k x / p}, \quad (2)$$

where  $F(y)$  is the Fourier transform of  $f(x)$ . Thus we see that the spectrum consists of a comb of discrete frequencies (comb lines) that are integer multiples of  $f_{rep}$ . The amplitude of each comb line is given by the spectrum of a single pulse evaluated at the frequency of the comb line.

Including a pulse-to-pulse phase shift,  $\Delta\phi_{ce}$ , means the pulses are not all identical, and the spectrum is not a simple Fourier series. Thus a bit more work is required to determine the spectrum. We write the electric field,  $E(t)$ , of a pulse train using the electric field of a single pulse  $E_p$  given above with  $\phi_{ce} = n\Delta\phi_{ce} + \phi_0$  for pulse  $n$ . Then  $E(t)$  for the train of pulses is

$$E(t) = \sum_n \hat{E}(t - n\tau) e^{i(\omega_c t - n\omega_c \tau + n\Delta\phi_{ce} + \phi_0)} = \sum_n \hat{E}(t - n\tau) e^{i(\omega_c t + n(\Delta\phi_{ce} - \omega_c \tau) + \phi_0)}. \quad (3)$$

Taking the Fourier transform, we obtain

$$E(\omega) = \int \sum_n \hat{E}(t - n\tau) e^{i(\omega_c t + n(\Delta\phi_{ce} - \omega_c \tau) + \phi_0)} e^{-i\omega t} dt = \sum_n e^{i(n(\Delta\phi_{ce} - \omega_c \tau) + \phi_0)} \int \hat{E}(t - n\tau) e^{-i[(\omega - \omega_c)t]} dt. \quad (4)$$

Defining  $\tilde{E}(\omega) = \int \hat{E}(t) e^{-i\omega t} dt$  and using the identity  $\int f(x - a) e^{-i\alpha x} dx = e^{-i\alpha a} \int f(x) e^{-i\alpha x} dx$  yields

$$\begin{aligned} E(\omega) &= \sum_n e^{i(n(\Delta\phi_{ce} - \omega_c \tau) + \phi_0)} e^{-in(\omega - \omega_c)\tau} \tilde{E}(\omega - \omega_c) = e^{i\phi_0} \tilde{E}(\omega - \omega_c) \sum_n e^{i(n\Delta\phi_{ce} - n\omega\tau)} \\ &= e^{i\phi_0} \tilde{E}(\omega - \omega_c) \sum_m \delta(\Delta\phi_{ce} - \omega\tau - 2\pi m) \end{aligned}, \quad (5)$$

where the last step is obtained by using Eq. (2) in reverse together with the fact that the Fourier

transform of  $\delta(t)$  is a constant. This is a comb spectrum with frequencies  $\omega_m = \frac{2m\pi}{\tau} - \frac{\Delta\phi_{ce}}{\tau}$  or,

converting from angular frequency,

$$\nu_m = mf_{rep} + f_0, \quad (6)$$

where  $f_0 = -\Delta\phi_{ce} \cdot f_{rep}/2\pi$  (note that it is common to drop the minus sign in this expression, which simply changes the sign in the definition of  $\Delta\phi_{ce}$ ). Hence we see that the position of the comb is offset from integer multiples of the repetition rate by the offset frequency,  $f_0$ , which is determined by the pulse-to-pulse phase shift. The connection between the time and frequency domain pictures is summarized in Fig. 2.

When we introduced the decomposition of the pulse into carrier and envelope, we noted that there are restrictions for a train of pulses. The carrier must have an integer number of cycles

between peaks of the electric field of successive pulses, as shown in Fig. 3. If the carrier wave with frequency  $\nu_c$  is described by  $\cos(2\pi\nu_c t)$ , the argument of the cosine must be equal to an integer multiple of  $2\pi$  when  $t$  equals the time between peaks of the electric field. This time is given by  $t = \tau + \frac{\Delta\phi_{CE}}{2\pi\nu_c}$  (see Fig 3). Plugging this in, we obtain a set of allowed carrier

frequencies  $m\nu_c = \frac{m}{\tau} - \frac{\Delta\phi_{CE}}{2\pi\tau} = mf_{rep} + f_0$ , i.e., the carrier frequency must be one of the comb

frequencies. This relationship is relaxed if a more complicated envelope is used, specifically if the envelope actually consists of several pulses. For example, if  $\Delta\phi_{CE} = \pi$ , and the envelope is chosen to describe two successive pulses with opposite sign, then the carrier frequency is shifted from the comb by  $f_{rep}/2$ . This may seem strange because there is no spectral content at the carrier frequency. However it is not surprising in the context of an amplitude modulation of a carrier, where there is no spectral content at the carrier frequency if a 100% bipolar modulation is used.

Examining a few simplified examples helps one to visualize the correspondence between the time and frequency domains. In Fig. 4, four spectra and their corresponding pulse trains are shown. The spectra consist of eight discrete lines. All times (frequencies) are normalized to the pulse period (repetition frequency). The comb lines are weighted by a Gaussian envelope centered at a frequency of  $10f_{rep}$ . In the time domain plots, both the envelope and carrier are also plotted. These examples are only illustrative as they correspond to an unrealistically high repetition rate such that only a few modes are within the spectral bandwidth of the laser.

The pulse-to-pulse change in the carrier-envelope phase,  $\Delta\phi_{ce}$ , of the pulse train emitted by a mode-locked laser arises from the difference between phase velocity,  $v_p$ , and group velocity,  $v_g$ , inside the laser cavity. For a round trip length  $L$ , the time it takes a pulse to make a round trip

is  $L/v_g$ , whereas for a phase front (e.g., a peak in the electric field) is  $L/v_p$ . The difference between these yields

$$\Delta\phi_{ce} = \omega_c L \left( \frac{1}{v_p} - \frac{1}{v_g} \right), \quad (7)$$

which corresponds to an offset frequency of

$$f_0 = \frac{\omega_c v_g}{2\pi} \left( \frac{1}{v_g} - \frac{1}{v_p} \right). \quad (8)$$

This relationship might be troubling at first glance as it appears that  $f_0$  depends on  $\omega_c$ , which can be chosen arbitrarily to be any comb line. However,  $v_p$  is by definition the phase velocity at  $\omega_c$  and thus depends on  $\omega_c$  because of dispersion. Explicitly including this dependence in equation (8) makes  $f_0$  independent of  $\omega_c$ .

### **Measurement and stabilization of $f_0$**

To fully characterize the frequencies of the comb lines, we need only measure two frequencies,  $f_{rep}$  and  $f_0$ , according to Eq. (6). Measurement of  $f_{rep}$  is straightforward; one simply illuminates a reasonably fast photodetector (typically a photodiode) with the pulse train and counts the frequency of the resulting electrical pulses with an ordinary frequency counter. Measuring  $f_0$  is a more difficult endeavor.

Given a source of optical radiation with known absolute frequency, one could imagine it would be easy to determine  $f_0$ . If such sources were readily available, then mode-locked lasers would not be useful for optical frequency metrology, this chapter would not have been written, and Jan Hall and Ted Hänsch would still be waiting for an early October call from Sweden.<sup>12</sup> However, as mentioned above, in order for a frequency to be “absolute,” it must be referenced to the frequency produced by a cesium clock at approximately 9 GHz. Spanning the gap of approximately 5 orders of magnitude from 9 GHz to optical frequencies was so challenging that sources of optical radiation with known frequency were very rare. However, the key point is that  $f_0$  can be determined without an optical frequency reference.

There are several methods for determining  $f_0$  without using an external reference.<sup>13</sup> The most common method is known as “self-referencing.”<sup>8</sup> Self-referencing provides a measurement of  $f_0$  without any external reference by comparing the spectral extremes of the comb through second harmonic generation. If the comb spectrum is sufficiently broad to covers an optical octave (factor of two in frequency), the second harmonic of the low-frequency (red) end of the comb will overlap with the high-frequency (blue) end. The heterodyne beat between the second harmonic and fundamental combs yields an rf frequency of

$$f_b = 2\nu_n - \nu_{2n} = 2(nf_{rep} + f_0) - (2nf_{rep} + f_0) = f_0 . \quad (9)$$

This simple equation is the key to self-referencing. Figure 5 gives a schematic representation of it by showing the fundamental and second harmonic combs. The figure is schematic because the entire comb is typically not doubled, but rather just a small portion of the spectrum is selected by phase matching in the second harmonic crystal.

An octave spanning spectrum would correspond to a transform limited pulse of 1 cycle in duration if it has a smooth spectrum, such as a Gaussian or  $\text{sech}^2(t)$  pulse. Single-cycle visible optical pulses have not been demonstrated, although mode-locked lasers have recently been demonstrated that produce octave spanning pulses with complicated spectra.<sup>14-17</sup> However, octave-spanning spectra can be produced by broadening the pulse spectrum external to the laser. This is done using self-phase modulation in a nonlinear media. Optical fiber is often used for this because the intensity is greatly increased by confining the light in a small core. For ordinary fiber and ultrashort pulses, the enhancement from confinement is counteracted by the effects of group velocity dispersion that cause the pulse to spread temporally, thereby lowering the peak intensity and hence decreasing the broadening.

The difficulty of obtaining an octave-spanning spectrum has been significantly reduced by the development of microstructured fiber,<sup>18</sup> which has made it possible to obtain bandwidth well in excess of an octave using the output from an ordinary (unamplified) mode-locked Ti:sapphire laser. Although the morphology of microstructure fiber is similar to that of photonic crystal fiber,<sup>19</sup> the essential physics only relies on the very small highly confined mode, as demonstrated by similar results obtained in fiber tapers.<sup>20</sup> Microstructure fibers consist of a fused silica core surrounded by air holes. This design yields a waveguide with a very high contrast of the effective index of refraction between core and cladding. The resultant waveguiding provides a long interaction length with a minimum beam cross section. In addition, the waveguide dispersion can cancel the material dispersion such that fiber can be designed with a zero point of the group velocity dispersion (GVD) within the operating spectrum of a Ti:sapph laser (for ordinary fiber the zero point of the group velocity dispersion can only occur for wavelengths longer than 1.3  $\mu\text{m}$ ). This dispersion property means that the pulse does not stretch in time as it

propagates, and the strong nonlinear interaction occurs over a relatively long distance (centimeters to meters, rather than millimeters in ordinary fiber). The output spectrum is very sensitive to the launched power and polarization. It is also sensitive to the spectral position relative to the zero-GVD point and the chirp of the incident pulse. Because the fiber displays anomalous dispersion, precompensation of the dispersion is not required if the laser spectrum is centered toward the long wavelength side of the zero dispersion point (i.e., in the anomalous dispersion region). Because the pulse is tuned close to the zero-GVD point, the output phase profile is dominated by third order dispersion.<sup>21</sup> Note that “higher-order” self-referencing techniques, for example, comparing 2<sup>nd</sup> harmonic to 3<sup>rd</sup> harmonic, have lower bandwidth requirements, however they are more complicated and require additional nonlinear conversion steps.<sup>17,22</sup>

Given our understanding of combs, self-referencing and how to generate an octave-spanning spectrum, we can now “build” an experimental apparatus for generating a stable frequency comb with a mode-locked laser, which is shown in Fig. 6. The comparison between  $\nu$  and  $2\nu$  is done by the portion inside the dashed box, which we will designate as a “ $\nu$ -to- $2\nu$  interferometer.” A typical RF spectrum of the signal produced by the photodiode is shown in Fig. 7. It is important that the reference signal be phase coherent with the repetition rate of the laser, otherwise even a very small frequency error can occur, which will cause  $\phi_{ce}$  to slip. For example, a 1 Hz error (i.e.,  $\sim 10^{-8}$  compared to the repetition rate) will cause a  $2\pi$  phase slip in 1 second. In Fig. 6 this is achieved by deriving the reference coherently from the repetition rate. This can also be achieved by using two frequency synthesizers running off a common time base and using one to lock  $f_{rep}$  and the other to lock  $f_0$ .<sup>23</sup>

In order to lock the comb, a laser parameter that influences  $\Delta\phi_{ce}$  is needed to implement active stabilization. This requires changing the difference between the round-trip group and phase delay inside the laser cavity. Two methods for doing this have been demonstrated: swiveling the end mirror of the laser cavity (see Fig. 14)<sup>24</sup> and adjusting the pump power.<sup>25</sup>

Rotating the end mirror of the laser arm that contains the prisms about a vertical axis (a swivel) produces a group delay for the intracavity pulse. This delay occurs because the different spectral components are spread out spatially across the mirror. The dispersion in the prisms results in a linear relationship between the spatial coordinate and the wavelength. Hence the mirror swivel provides a linear phase with frequency, which is equivalent to a group delay.<sup>26</sup> The group delay depends linearly on angle for small angles. The angle by which the mirror is swiveled is very small, approximately  $10^{-4}$  rad and thus does not appreciably change the cavity alignment. Since mechanical movement of the mirror is required, only limited servo bandwidth can be obtained using this method, which restricts how accurately  $f_0$  can be locked.

The physical origin of  $f_0$  depending on the pump intensity is not completely understood, although it is sufficiently well characterized to be a useful control knob.<sup>25,27,28</sup> When first observed, this effect was attributed to a combination of the nonlinear phase shift in the gain crystal (the Kerr effect) and group velocity dispersion coupled with frequency shifts.<sup>29</sup> However, the group velocity also depends on intensity, but with the opposite sign, which can reverse the effect.<sup>30</sup> Furthermore the fact that the dispersion in the cavity is not a fixed value, but there are compensating positive and negative dispersion regions reduces the sensitivity to intensity.<sup>31</sup> And finally, pulse reshaping can influence the apparent intensity dependent phase shift.<sup>32</sup>

## Optical frequency metrology with combs

The use of optical frequency combs to directly measure an optical frequency referenced to an rf clock is shown in Fig. 8. Since both  $f_r$  and  $f_0$  are rf frequencies, they are easily measured using a Cs clock as a reference. These measurements determine the frequencies of the optical comb lines based on Eq. (6). The optical frequency of interest (typically a single frequency laser locked to a molecular, atomic, or ionic transition) is now compared to the nearest comb line. This comparison is easily done by measuring the frequency of the heterodyne beat between them. If the heterodyne beat has frequency  $f_b$ , then the optical frequency is

$$f_{opt} = nf_r \pm f_0 \pm f_b. \quad (10)$$

The determination of  $n$  and whether to use the + or – can often be made based on a low resolution measurement of  $f_{opt}$ ; a standard commercial wavemeter is often sufficient. Lacking a low resolution measurement, these parameters can also be determined by systematically varying  $f_r$  and  $f_0$  and observing how  $f_b$  changes. The success of this method is due to its simplicity.

An example of optical frequency metrology using frequency combs is shown in Fig. 9. These data show measurements of the frequency of the  $^1S_0 - ^3P_0$  transition in  $^{87}\text{Sr}$  atoms that have been cooled to a temperature of approximately 1  $\mu\text{K}$ .<sup>33</sup> The fluctuations in the measurement gave an uncertainty of only 2.8 Hz whereas the systematic uncertainties amounted to 19 Hz. Further improvements have lowered the statistical uncertainty by close to another order of magnitude.

The remarkable impact of femtosecond comb technology on optical frequency metrology is shown in Figure 10, which shows the historical trend in measurement uncertainty.

Femtosecond frequency combs were introduced in 2000, clearly causing an abrupt decrease in the frequency uncertainty. The current uncertainties are approaching those of the best Cs clocks in the world.

### **Optical Atomic Clocks**

The attraction of optical clocks is simple: the uncertainty in a time/frequency measurement is inversely related to the number of cycles counted. Thus increasing the frequency allows the same uncertainty to be achieved in a much shorter time. For example, Cs clocks require several weeks of averaging to achieve an uncertainty of  $10^{-15}$ . A clock using an optical frequency transition can achieve the same uncertainty in a few seconds. The idea that a laser locked to a narrow molecular, atomic, or ionic transition is effectively an optical atomic clock is not a new one.<sup>34</sup> However, producing a useable rf output signal encountered the same obstacles mentioned above for absolute optical frequency metrology, namely linking radio and optical frequencies.

The simplest implementation of an optical atomic clock using a femtosecond comb consists of locking  $f_0 = 0$  and the  $n^{\text{th}}$  comb line to the frequency of an atomic transition,  $\nu_a$ . The rf clock signal is  $f_r = \nu_a/n$ , which can simply be detected with a photodiode to produce an electrical signal. More complicated schemes have also been used.

An example of the conversion from optical to radio frequency is shown in Fig. 11.<sup>35</sup> The vertical scale shows the Allan deviation, which is a measure of the instability of a signal of nominally constant frequency. If the fluctuations in the frequency are random, then the instability should decrease with increasing averaging time (gate time). However if there is a systematic drift in the frequency then this will not be the case for larger averaging times. In the study presented in Fig. 11, two optical frequency combs were locked to CW lasers that were in turn locked to

optical cavities (in order to determine if a clock is fluctuating, it must always be compared to a second clock). At short gate times, the instability decreases with increasing gate time. At longer averaging times, drift of the physical length of cavities dominates and the instability no longer decreases. These results show that for short averaging times, the mode-locked laser based combs generate more stable rf signals than a hydrogen maser. Furthermore, curve (f) shows that the optical signals are more stable than the rf frequencies, suggesting that further improvement is possible.

Early examples of optical clocks used a single Hg ion<sup>36</sup> and molecular iodine<sup>37</sup> as the standards. The single Hg ion provides a high stability, whereas molecular iodine is a simpler implementation that could be used in a portable clock. Other possible standards include cold neutral Ca<sup>38,39</sup> and Sr<sup>+</sup>.<sup>40</sup> Studies show that the intrinsic stability of the comb reaches the  $10^{-19}$  level,<sup>41</sup> suggesting that clocks are limited by the atomic standard, not the comb. One of the more exciting recent developments has been the use of atoms trapped in an optical lattice,<sup>42</sup> which promises to combine the best features of ion and cold atom standards.<sup>33,43</sup> A review can be found in the paper by Gill.<sup>44</sup>

### **Other aspects of carrier-envelope phase**

The development of techniques to stabilize the frequency comb produced by mode-locked lasers has also had a tremendous impact on high intensity experiments that are sensitive to electric field of the pulse. Generally, these types of experiments involve ionization of an atom (or molecule) by an intense short optical pulse via tunneling through the Coulomb barrier.<sup>45</sup> Either the ionized electrons are directly detected, or the short wavelength radiation emitted when they collide with ionic core is observed. The latter case is known as “high harmonic generation.” The spectrum of

odd harmonics can be thought of as arising from interference between the radiation from each half-cycle of the driving near-infrared pulse. The radiation from each half cycle actually consists of a subfemtosecond burst in the extreme ultraviolet through soft x-ray spectral region. By using optical pulses with controlled carrier-envelope phase, it is possible to generate single “attosecond” pulses.<sup>46</sup>

### **Summary**

The ability to control the carrier-envelope phase evolution in mode-locked lasers to produce optical frequency combs has produced a revolutionary advance in the field of optical frequency metrology. Indeed, the measurement of frequencies up through the visible range is no longer a field of active research, but rather a “solved problem.” The frontier is now moving into the ultraviolet region of the spectrum. Furthermore, optical frequency combs already serve as the “clockwork” in a new generation of atomic clocks that rely on optical frequency quantum transitions. Already these optical atomic clocks are rivaling the best cesium fountain clocks in terms of frequency stability.

## Problems

- 1) The frequency modes of a laser cavity are given by the standard formula for a Fabry-Perot cavity,  $\omega_m = \frac{2\pi c}{nL} m$ , which only includes the index of refraction. Our derivation of the spacing of the comb lines relies on the time between pulses, which is determined by the group velocity inside the cavity. In any dispersive material, the group velocity will not necessarily match the phase velocity, suggesting that these two approaches give different comb spacings. Show that they do not. The only assumption you need make is that there is no net group velocity dispersion inside the cavity. Furthermore, you should find that the modes of a Fabry-Perot cavity that satisfy these condition have exactly the frequencies we derived, including the offset frequency.
- 2) An alternative approach to calculating the spectrum is to consider the excitation of a narrow resonance such as atomic absorption line. If the coherence time is sufficiently long such that the resonance remembers the phase of the previous pulse when the next one in the train arrives, the effect of the pulses can either be constructive, increasing the excitation level, or destructive, decreasing the excitation level. Calculate the frequencies for which the interference is constructive for a pulse train with a pulse-to-pulse slip of  $\Delta\phi_{ce}$  and show that they correspond to the frequencies of the comb lines.
- 3) A nonlinear crystal with a second order nonlinearity produces an output field  $E_o \sim \chi^{(2)} E_i^2$  where  $E_i$  is the input field and  $\chi^{(2)}$  is the nonlinear susceptibility (just consider it a given constant for this problem). If the input field is a simple harmonic wave, the output field is at twice the frequency, and thus such crystals are often called “second

harmonic crystals.” What is the spectrum of the output field if the input field is a pulse train with spacing  $1/f_{\text{rep}}$  and pulse-to-pulse carrier-envelope  $\Delta\phi_{ce}$ ? Why?

## Figure captions

Fig. 1. An ultrashort optical pulse (thick solid line) showing the carrier (dashed line) and envelope (thin solid line).

Fig. 2. Time-frequency correspondence and relationship between  $\Delta\phi_{CE}$  and  $f_0$ . (a) In the time domain, the relative phase between the carrier and the envelope evolves from pulse to pulse by the amount  $\Delta\phi_{CE}$ . (b) In the frequency domain, the elements of the frequency comb of a mode-locked pulse train are spaced by  $f_{rep}$ . The entire comb is offset from integer multiples of  $f_{rep}$  by an offset frequency  $f_0 = \Delta\phi_{rep}/2\pi$ . Without active stabilization,  $f_0$  is a dynamic quantity, which is sensitive to perturbation of the laser.

Fig. 3. Schematic used to derive allowed carrier frequencies. The carrier must line up with the peak of the electric field in successive pulses. The time between peaks is given by the time between pulses plus the pulse-to-pulse phase shift,  $\Delta\phi_{ce}$ .

Fig. 4. Examples of the correspondence between time and frequency domain pictures. The frequency spectrum is shown on the left and the corresponding pulse train on the right. All times and frequencies are normalized to the repetition rate. The bottom two panels differ by an overall phase shift of  $\pi/8$ , which does not change the frequency spectrum but does change the temporal dependence. In the right hand panels, the red line shows the carrier and the blue line the envelope.

Fig. 5. Schematic of the self-referencing technique for determining the offset frequency of the frequency comb produced by a femtosecond mode-locked laser. The frequency difference between the fundamental comb and its second harmonic is the offset frequency. In the region where overlap occurs, this is easily detected as a heterodyne beat.

Fig. 6. Experimental setup for stabilizing the frequency comb of a mode-locked laser. The fs laser is located inside the shaded box. Solid lines are optical paths, and dashed lines are electrical paths. The high reflector mirror is mounted on a transducer to provide both tilt and translation. AOM, acousto-optic modulator;; SHX, second harmonic crystal.

Fig. 7. Typical experimental RF spectrum of the output of the photodiode showing both repetition rate signal and heterodyne beats due to  $\nu$ -to- $2\nu$  interference.

Fig. 8. Schematic showing use of frequency combs in optical frequency metrology.

Fig 9. Accumulated record of the  $^{87}\text{Sr } ^1S_0 - ^3P_0$  optical clock transition frequency. Each entry is a weighted mean of several independent measurements that are referenced to the NIST Cs fountain clock. [courtesy of Jun Ye, JILA]

Fig. 10. Historical progress in absolute optical frequency measurements (courtesy of Leo Hollberg, NIST-Boulder).

Fig. 11. Allan deviation measurements taken at microwave (filled symbols) and optical (open symbols) carrier frequencies: Curve a,  $\sigma_{y,10\text{GHz}}(\tau)$  when the 10-GHz signals are synthesized from two independent cavity-stabilized cw lasers; curve b, instability of the 657-nm cw laser; curve c, current demonstrated upper limit for the NIST Ca and Hg<sup>+</sup>-ion optical frequency standards; curve d, residual  $\sigma_{y,10\text{GHz}}(\tau)$  when a common optical reference is used; curve e, state-of-the-art hydrogen maser; curve f, frequency combs in the optical domain. [From Bartels, et al., Opt. Lett. 30, 667 (2005)].

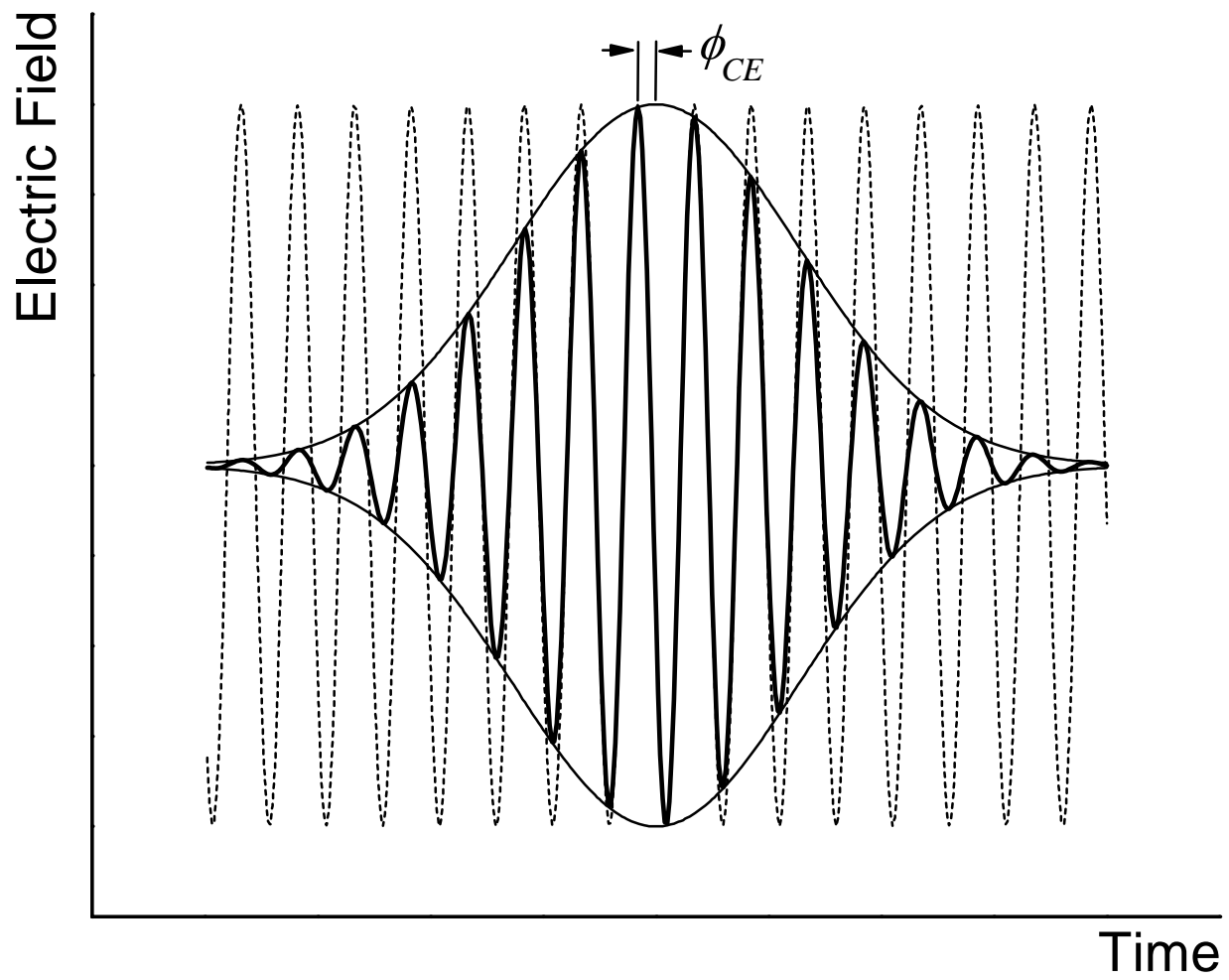


Figure 1

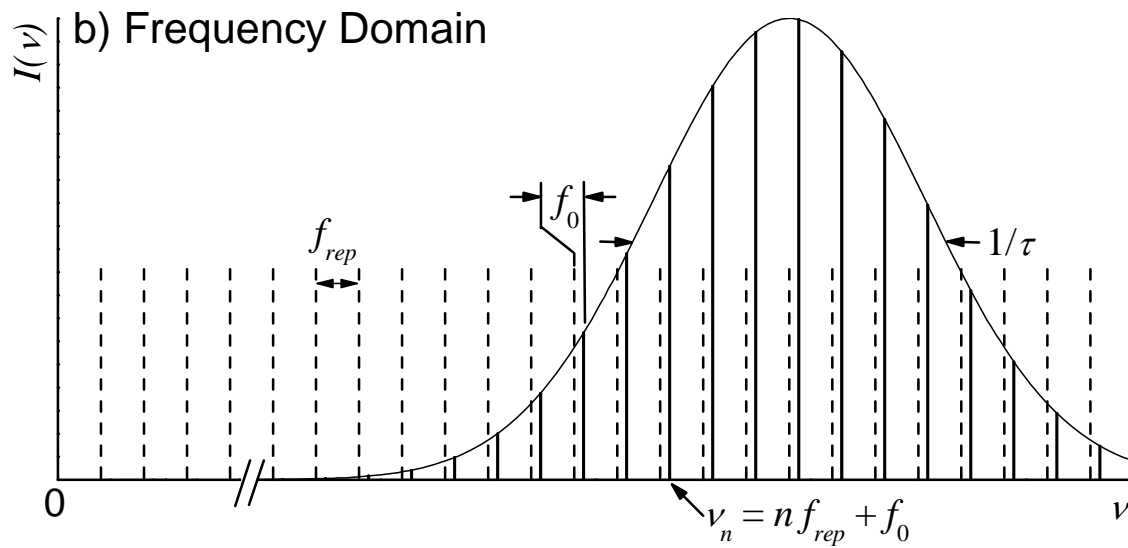
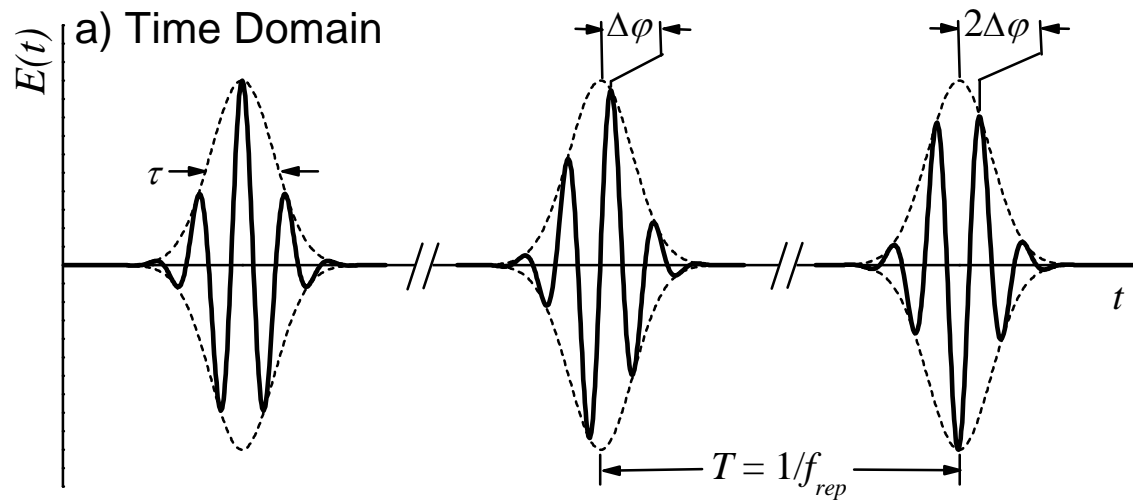


Figure 2

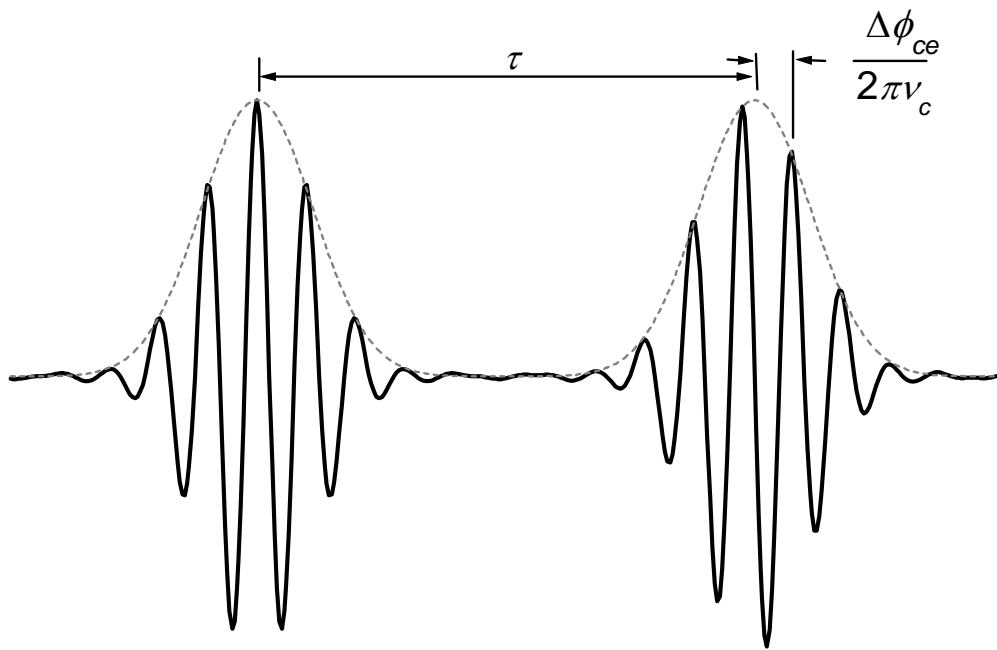


Figure 3

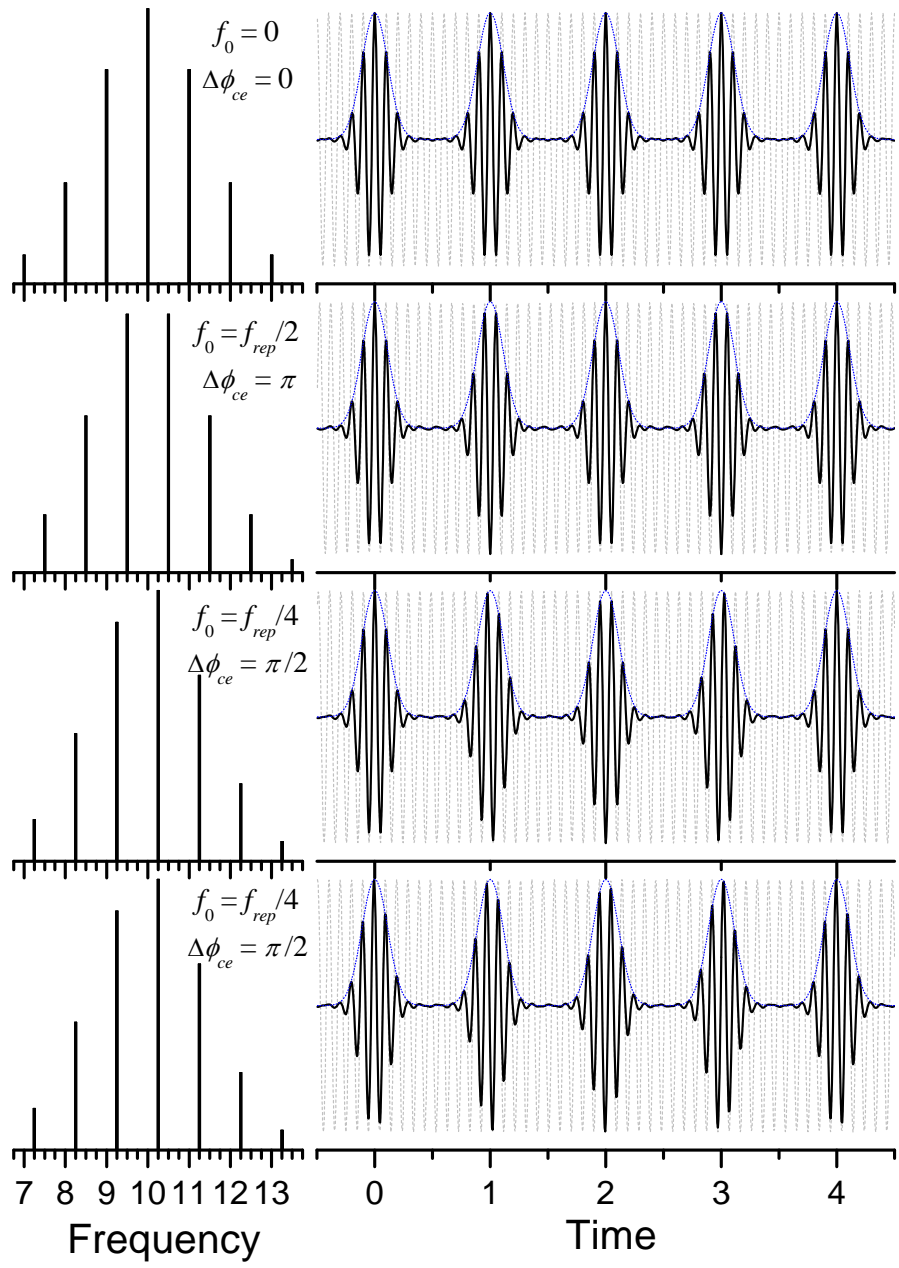
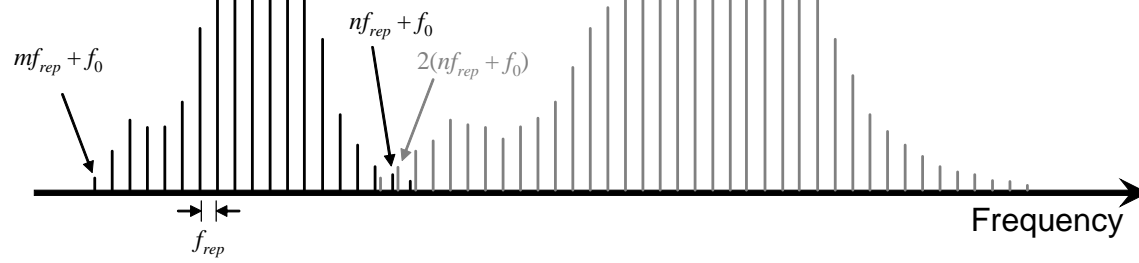


Figure 4

Fundamental  
Spectrum  
Figure 5

Second Harmonic  
Spectrum



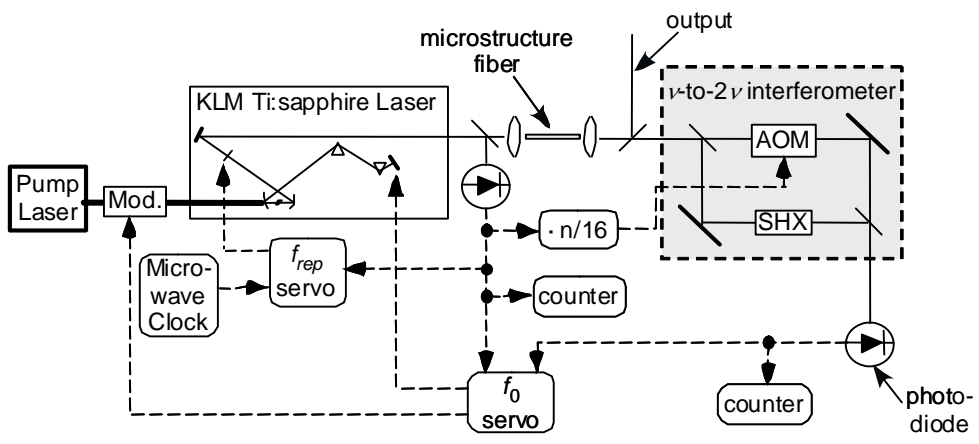


Figure 6

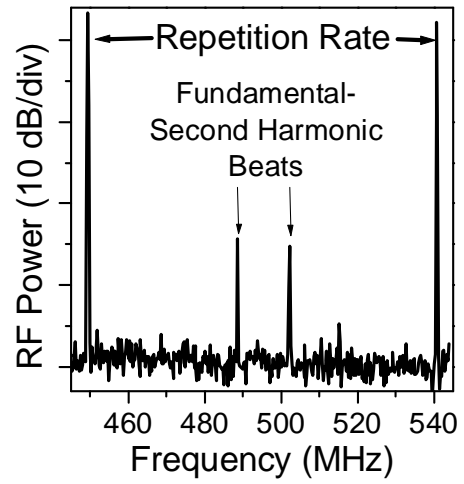


Figure 7.

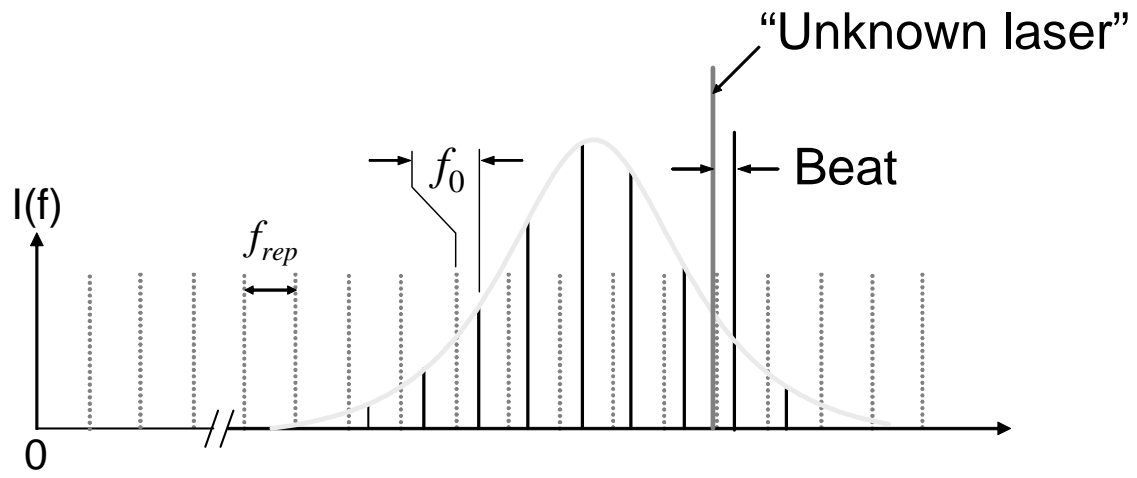


Fig. 8.

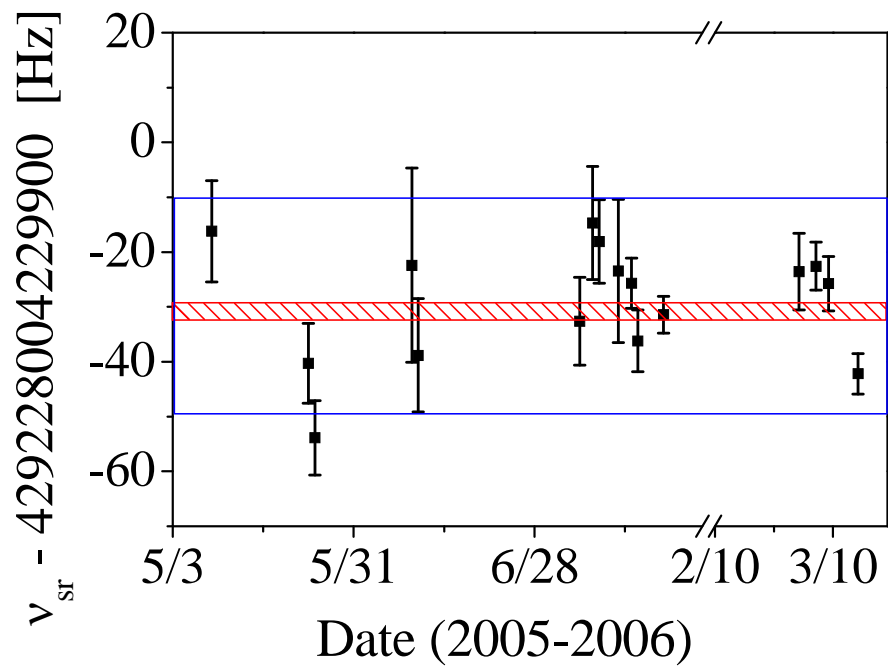


Fig. 9.

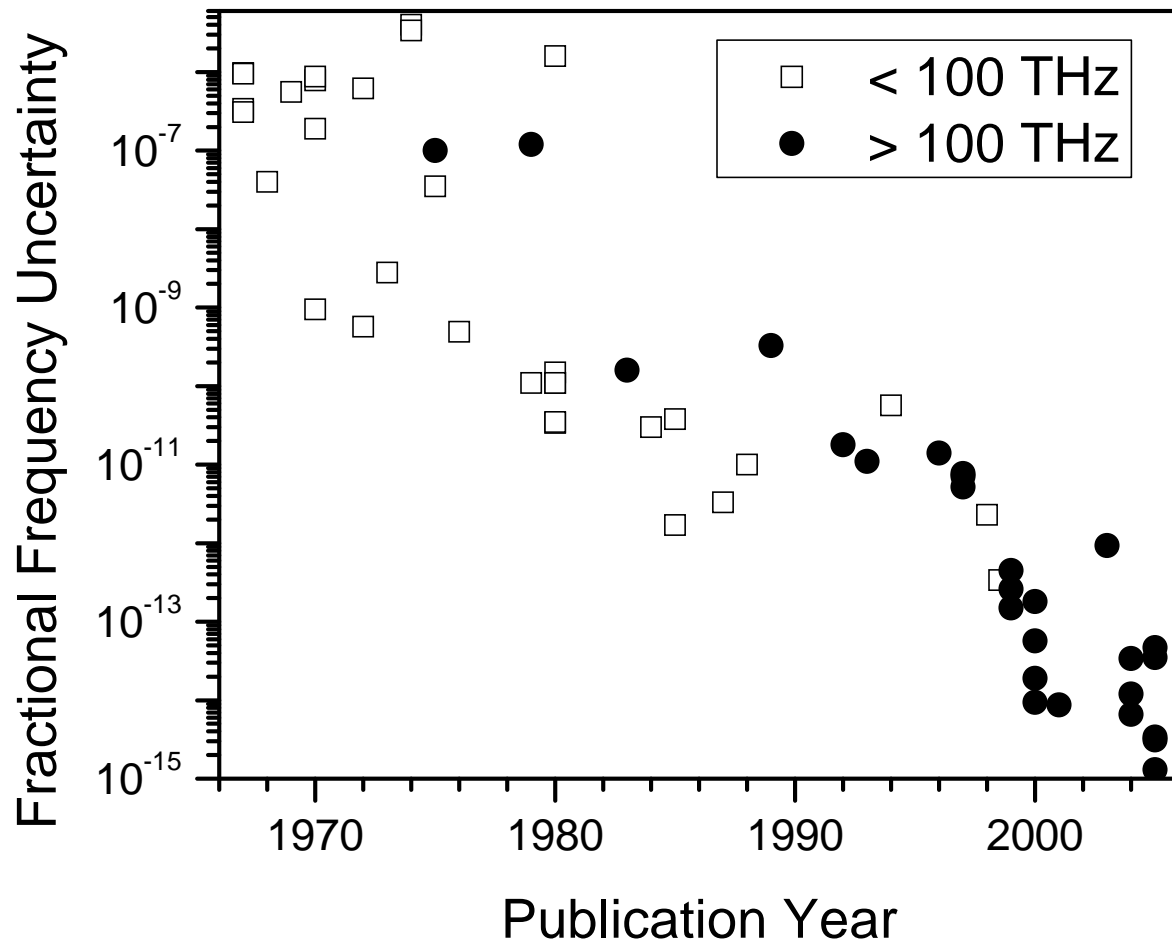


Fig 10.

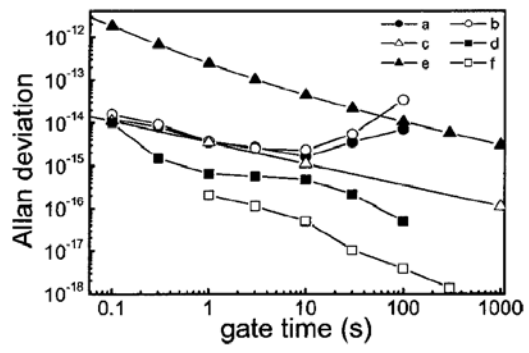


Fig. 11.

## References

- 1 Y. V. Baklanov and V. P. Chebotayev, "Narrow Resonances of 2-Photon Absorption of Super-Narrow Pulses in a Gas," *Applied Physics* **12**, 97-99 (1977).
- 2 J. N. Eckstein, A. I. Ferguson, and T. W. Hänsch, "High-Resolution 2-Photon Spectroscopy with Picosecond Light-Pulses," *Phys. Rev. Lett.* **40**, 847-850 (1978).
- 3 M. Kourogi, K. Nakagawa, and M. Ohtsu, "Wide-Span Optical Frequency Comb Generator for Accurate Optical Frequency Difference Measurement," *IEEE J. Quantum Electron.* **29**, 2693-2701 (1993).
- 4 T. Udem, J. Reichert, T. W. Hänsch, and M. Kourogi, "Absolute optical frequency measurement of the cesium D-2 line," *Phys. Rev. A* **62**, 031801 (2000).
- 5 S. T. Cundiff, J. Ye, and J. L. Hall, "Optical frequency synthesis based on mode-locked lasers," *Rev. Sci. Instr.* **72**, 3749-3771 (2001).
- 6 S. A. Diddams, D. J. Jones, J. Ye, S. T. Cundiff, J. L. Hall, J. K. Ranka, R. S. Windeler, R. Holzwarth, T. Udem, and T. W. Hänsch, "Direct link between microwave and optical frequencies with a 300 THz femtosecond laser comb," *Phys. Rev. Lett.* **84**, 5102-5105 (2000).
- 7 R. Holzwarth, T. Udem, T. W. Hänsch, J. C. Knight, W. J. Wadsworth, and P. S. J. Russell, "Optical frequency synthesizer for precision spectroscopy," *Phys. Rev. Lett.* **85**, 2264-2267 (2000).
- 8 D. J. Jones, S. A. Diddams, J. K. Ranka, A. Stentz, R. S. Windeler, J. L. Hall, and S. T. Cundiff, "Carrier-envelope phase control of femtosecond mode-locked lasers and direct optical frequency synthesis," *Science* **288**, 635-639 (2000).
- 9 K. M. Evenson, J. S. Wells, F. R. Petersen, B. L. Danielson, and G. W. Day, "Accurate Frequencies of Molecular Transitions Used in Laser Stabilization - 3.39  $\mu\text{m}$  Transition in  $\text{CH}_4$  and 9.33  $\mu\text{m}$  and 10.18  $\mu\text{m}$  Transitions in  $\text{CO}_2$ ," *App. Phys. Lett.* **22**, 192-195 (1973).
- 10 H. Schnatz, B. Lipphardt, J. Helmcke, F. Riehle, and G. Zinner, "First phase-coherent frequency measurement of visible radiation," *Phys. Rev. Lett.* **76**, 18-21 (1996).
- 11 L. Mandel and E. Wolf, *Optical coherence and quantum optics* (Cambridge University Press, New York, 1995).
- 12 [http://nobelprize.org/nobel\\_prizes/physics/laureates/2005/](http://nobelprize.org/nobel_prizes/physics/laureates/2005/).
- 13 H. R. Telle, G. Steinmeyer, A. E. Dunlop, J. Stenger, D. H. Sutter, and U. Keller, "Carrier-envelope offset phase control: A novel concept for absolute optical frequency measurement and ultrashort pulse generation," *Appl. Phys. B* **69**, 327-332 (1999).
- 14 T. M. Fortier, A. Bartels, and S. A. Diddams, "Octave-spanning Ti: sapphire laser with a repetition rate  $> 1$  GHz for optical frequency measurements and comparisons," *Opt. Lett.* **31**, 1011-1013 (2006).
- 15 T. M. Fortier, D. J. Jones, and S. T. Cundiff, "Phase stabilization of an octave-spanning Ti: sapphire laser," *Opt. Lett.* **28**, 2198-2200 (2003).
- 16 L. Matos, D. Kleppner, O. Kuzucu, T. R. Schibli, J. Kim, E. P. Ippen, and F. X. Kärtner, "Direct frequency comb generation from an octave-spanning, prismless Ti: sapphire laser," *Opt. Lett.* **29**, 1683-1685 (2004).
- 17 U. Morgner, R. Ell, G. Metzler, T. R. Schibli, F. X. Kärtner, J. G. Fujimoto, H. A. Haus, and E. P. Ippen, "Nonlinear optics with phase-controlled pulses in the sub-two-cycle regime," *Phys. Rev. Lett.* **86**, 5462-5465 (2001).

18 J. K. Ranka, R. S. Windeler, and A. J. Stentz, "Visible continuum generation in air-silica  
microstructure optical fibers with anomalous dispersion at 800 nm," *Opt. Lett.* **25**, 25-27  
(2000).

19 J. C. Knight, J. Broeng, T. A. Birks, and P. S. J. Russel, "Photonic band cap guidance in  
optical fibers," *Science* **282**, 1476-1478 (1998).

20 T. A. Birks, W. J. Wadsworth, and P. S. Russell, "Supercontinuum generation in tapered  
fibers," *Opt. Lett.* **25**, 1415-1417 (2000).

21 Q. Cao, X. Gu, E. Zeek, M. Kimmel, R. Trebino, J. Dudley, and R. S. Windeler,  
"Measurement of the intensity and phase of supercontinuum from an 8-mm-long  
microstructure fiber," *Appl. Phys. B* **77**, 239-244 (2003).

22 T. M. Ramond, S. A. Diddams, L. Hollberg, and A. Bartels, "Phase-coherent link from  
optical to microwave frequencies by means of the broadband continuum from a 1-GHz  
Ti: sapphire femtosecond oscillator," *Opt. Lett.* **27**, 1842-1844 (2002).

23 A. Apolonski, A. Poppe, G. Tempea, C. Spielmann, T. Udem, R. Holzwarth, T. W.  
Hänsch, and F. Krausz, "Controlling the phase evolution of few-cycle light pulses," *Phys.*  
*Rev. Lett.* **85**, 740-743 (2000).

24 T. Udem, J. Reichert, R. Holzwarth, and T. W. Hänsch, "Absolute optical frequency  
measurement of the cesium D-1 line with a mode-locked laser," *Phys. Rev. Lett.* **82**,  
3568-3571 (1999).

25 A. Poppe, R. Holzwarth, A. Apolonski, G. Tempea, C. Spielmann, T. W. Hänsch, and F.  
Krausz, "Few-cycle optical waveform synthesis," *Appl. Phys. B* **72**, 373-376 (2001).

26 K. F. Kwong, D. Yankelevich, K. C. Chu, J. P. Heritage, and A. Dienes, "400-Hz  
Mechanical Scanning Optical Delay-Line," *Opt. Lett.* **18**, 558-560 (1993).

27 K. W. Holman, R. J. Jones, A. Marian, S. T. Cundiff, and J. Ye, "Detailed studies and  
control of intensity-related dynamics of femtosecond frequency combs from mode-locked  
Ti: sapphire lasers," *IEEE J. Sel. Top. Quantum Electron.* **9**, 1018-1024 (2003).

28 K. W. Holman, R. J. Jones, A. Marian, S. T. Cundiff, and J. Ye, "Intensity-related  
dynamics of femtosecond frequency combs," *Opt. Lett.* **28**, 851-853 (2003).

29 L. Xu, C. Spielmann, A. Poppe, T. Brabec, F. Krausz, and T. W. Hänsch, "Route to phase  
control of ultrashort light pulses," *Opt. Lett.* **21**, 2008-2010 (1996).

30 H. A. Haus and E. P. Ippen, "Group velocity of solitons," *Opt. Lett.* **26**, 1654-1656  
(2001).

31 M. J. Ablowitz, B. Ilan, and S. T. Cundiff, "Carrier-envelope phase slip of ultrashort  
dispersion-managed solitons," *Opt. Lett.* **29**, 1808-1810 (2004).

32 P. M. Goorjian and S. T. Cundiff, "Nonlinear effects on the carrier-envelope phase," *Opt.*  
*Lett.* **29**, 1363-1365 (2004).

33 A. D. Ludlow, M. M. Boyd, T. Zelevinsky, S. M. Foreman, S. Blatt, M. Notcutt, T. Ido,  
and J. Ye, "Systematic study of the Sr-87 clock transition in an optical lattice," *Phys. Rev.*  
*Lett.* **96**, 033003 (2006).

34 V. P. Chebotayev, V. G. Goldort, V. M. Klementyev, M. V. Nikitin, B. A. Timchenko,  
and V. F. Zakharyash, "Development of an Optical-Time Scale," *Appl. Phys. B* **29**, 63-65  
(1982).

35 A. Bartels, S. A. Diddams, C. W. Oates, G. Wilpers, J. C. Bergquist, W. H. Oskay, and L.  
Hollberg, "Femtosecond-laser-based synthesis of ultrastable microwave signals from  
optical frequency references," *Opt. Lett.* **30**, 667-669 (2005).

- 36 S. A. Diddams, T. Udem, J. C. Bergquist, E. A. Curtis, R. E. Drullinger, L. Hollberg, W.  
M. Itano, W. D. Lee, C. W. Oates, K. R. Vogel, and D. J. Wineland, "An optical clock  
based on a single trapped Hg-199(+) ion," *Science* **293**, 825-828 (2001).
- 37 J. Ye, L. S. Ma, and J. L. Hall, "Molecular iodine clock," *Phys. Rev. Lett.* **87**, 270801  
(2001).
- 38 T. Udem, S. A. Diddams, K. R. Vogel, C. W. Oates, E. A. Curtis, W. D. Lee, W. M. Itano,  
R. E. Drullinger, J. C. Bergquist, and L. Hollberg, "Absolute frequency measurements of  
the Hg+ and Ca optical clock transitions with a femtosecond laser," *Phys. Rev. Lett.* **86**,  
4996-4999 (2001).
- 39 G. Wilpers, T. Binnewies, C. Degenhardt, U. Sterr, J. Helmcke, and F. Riehle, "Optical  
clock with ultracold neutral atoms," *Phys. Rev. Lett.* **89**, 230801 (2002).
- 40 H. S. Margolis, G. P. Barwood, G. Huang, H. A. Klein, S. N. Lea, K. Szymaniec, and P.  
Gill, "Hertz-level measurement of the optical clock frequency in a single Sr-88(+) ion,"  
*Science* **306**, 1355-1358 (2004).
- 41 L. S. Ma, Z. Y. Bi, A. Bartels, L. Robertsson, M. Zucco, R. S. Windeler, G. Wilpers, C.  
Oates, L. Hollberg, and S. A. Diddams, "Optical frequency synthesis and comparison  
with uncertainty at the  $10^{-19}$  level," *Science* **303**, 1843-1845 (2004).
- 42 M. Takamoto, F. L. Hong, R. Higashi, and H. Katori, "An optical lattice clock," *Nature*  
**435**, 321-324 (2005).
- 43 Z. W. Barber, C. W. Hoyt, C. W. Oates, L. Hollberg, A. V. Taichenachev, and V. I.  
Yudin, "Direct excitation of the forbidden clock transition in neutral Yb-174 atoms  
confined to an optical lattice," *Phys. Rev. Lett.* **96**, 083002 (2006).
- 44 P. Gill, "Optical frequency standards," *Metrologia* **42**, S125-S137 (2005).
- 45 P. B. Corkum, "Plasma Perspective on Strong-Field Multiphoton Ionization," *Phys. Rev.*  
*Lett.* **71**, 1994-1997 (1993).
- 46 R. Kienberger, M. Uiberacker, E. Goulielmakis, A. Baltuska, M. Drescher, and F. Krausz,  
"Single sub-fs soft-X-ray pulses: generation and measurement with the atomic transient  
recorder," *J. Mod. Opt.* **52**, 261-275 (2005).